Towards a grain-scale modeling of crack initiation in rolling contact fatigue - Part 2: Persistent slip band modeling

Lucas Fourel, Jean-Philippe Noyel, Etienne Bossy, Xavier Kleber, Philippe Sainsot, Fabrice Ville

Towards a Grain-scale Modeling of Crack Initiation in Rolling Contact Fatigue - Part 2: Persistent Slip Band Modeling

Lucas Fourel[a,b,c], Jean-Philippe Noyel[b], Etienne Bossy[b], Xavier Kleber[c], Philippe Sainsot[a] and Fabrice Ville[a,*]

[a] Univ Lyon, INSA Lyon, CNRS, LaMCoS, UMR5259, 69621 Villeurbanne, France
[b] Univ Lyon, ECAM Lyon, LabECAM, F-69005 Lyon, France
[c] Univ Lyon, INSA Lyon, MATEIS, UMR CNRS 5510, F-69621 Villeurbanne, France

ARTICLE INFO

Keywords:
Rolling contact
Fatigue
Mesoscopic
Numerical analysis

ABSTRACT

Rolling Contact Fatigue (RCF) is the result of crack initiation and propagation leading to surface damages. This study proposes a mesoscopic model for RCF crack initiation simulation. Finite Element Method (FEM) is used to obtain stresses using cubic elasticity. Persistent Slip Bands (PSBs) are modeled using polycrystalline geometry and grain orientations. PSBs can pass through Grain Boundaries (GBs) if the misorientation of the adjacent grains is lower than a critical angle. The Tanaka-Mura micromechanical model is then used to calculate the number of loading cycles required to initiate cracks. The results are compared to previous models and experiments. Initiation depths appear to be consistent.

1. Introduction

Rolling Contact Fatigue (RCF) concerns most of the components that endure repeated contact pressure such as rolling bearings, gears or railway tracks. Historically, the service life of these components was determined by empirical models such as Wöhler curves [1] or Coffin-Manson law [2, 3]. ISO 281 is a current standard which is used to predict the service life of rolling bearings, it is based on Lundberg and Palmgren's works [4, 5] which also arise from experimental results. In the early 1980's, researchers have started to adopt deterministic approaches in order to predict service life based on the actual physical mechanisms that cause fatigue [6]. RCF modeling was then separated into two categories of models: models treating crack initiation and models treating crack propagation although some studies combined both [7]. Concerning crack initiation, the role of the microstructure of the materials is all the more important, as in this case the deterioration processes are very often associated with microstructural changes [6]. Physical phenomena operate at the atomic scale which makes a complete nanoscale model extremely hard to develop and compute.

Some researchers have nonetheless developed micromechanical model based on fatigue physics in order to evaluate number of cycles to crack initiation (or fatigue crack threshold) as a function of stresses based on simplifying assumptions. This is the case of Tanaka and Mura who developed a fatigue crack initiation law based on the assumption that crack initiation is a result of dislocation slip and accumulation [8]. As first pointed out by Ewing and Humphrey [9], dislocations form Persistent Slip Bands (PSBs) which are preferred locations for plastic strain. Dörr and Blochwitz [10, 11, 12] and then Zhang and Wang [13, 14, 15] studied this theory and extended the knowledge concerning fatigue crack initiation at PSBs. The Tanaka-Mura model is particularly interesting because it is physically based and it can be easily implemented into a numerical model in combination with stress field computation. Several studies used Tanaka-Mura to predict fatigue crack threshold for structural fatigue. Bruckner-Foit et al. [16, 17] studied the fatigue crack threshold on martensitic steel and Toyoda et al. [18] on thin-walled high strength steel. Hilgendorff et al. [19] used a boundary element method to compute stresses and Briffod et al. [20] used a crystal plasticity model in combination with the Tanaka-Mura model in pure α-iron.

In this study, Tanaka-Mura's law is used in order to simulate crack initiation in RCF which differs from structural fatigue on multiple aspects [6, 21]. In RCF, the stress state is multi-axial and non-proportional, moreover, stresses are highly localized at the contact region. These specific conditions are one of the main reasons to model crack initiation at a mesoscopic length scale to account for the most fundamental principles of fatigue. Raje et al. developed a mesoscopic statistical model to estimate life scatter in RCF [22]. This model use the random nature of the material microstructure as a cause of the Weibull distribution of fatigue life. They found very good agreement with experimental data. Starting from the same idea that mesoscopic modeling is the key to explain the complexity of RCF, this paper proposes a grain-scale numerical model. This model focuses on the elementary principle of fatigue that large scale damages result from smaller scale defect accumulation and propagation.

In a previous study [23], an isotropic model was developed using Tanaka-Mura's approach to predict crack initiation in rolling contact fatigue. This article goes further in the modeling of the physics of fatigue crack initiation.

In the next section, physics of fatigue crack initiation and the Tanaka-Mura micromechanical model are described. Then, the numerical model is presented along with the polycrystalline geometry and the anisotropic properties. Finally,

*Corresponding author
fabrice.ville@insa-lyon.fr (F. Ville)
ORCID(s): 0000-0002-9743-8820 (F. Ville)

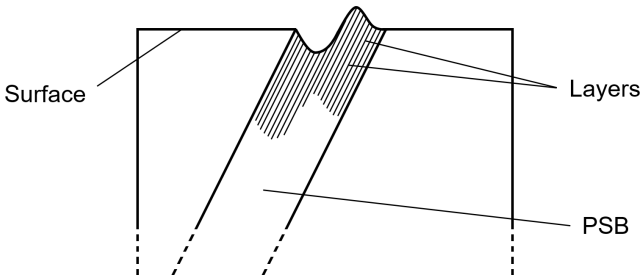

Figure 1: Persistent Slip Band (PSB) inducing intrusions and extrusions at the free surface of the material.

shear stress range calculation is detailed and a method to model PSBs in polycrystals is proposed.

2. Physics of Fatigue Crack Initiation

Sangid's review article [24] provides extensive explanation on fatigue crack initiation. The main physical aspects on which the following numerical model is based are described in this section. Fatigue is characterised by series of forward and reverse loading. This repeated loading induces stresses in the material which may cause micro-plasticity at certain favorable locations [24], and shear stress is widely recognized to be the primary cause [21]. In order to minimize the energy of the material structure exposed to shear stress, dislocations form, move via slip and accumulate forming more stable configurations [25]. These phenomena are the core principles of plastic deformation in metals. In crystalline materials, the dislocation slip can be concentrated into Persistent Slip Bands (PSBs) [9] because they constitute preferred locations for slip due to softening [26]. Even though PSBs appear only under certain conditions, they have been observed in most face-centered cubic (fcc) and body-centered cubic (bcc) materials [27]. PSBs seem to not occur at very high temperature (above one-half of the melting temperature [28]) and only for a nearly symmetrical loading [27]. However, they still constitute the most common location for fatigue crack initiation in polycrystalline materials [24, 26, 27]. PSBs under contact fatigue conditions have been observed by Forster et al. [29] in steel and by Medina et al. [30] in bronze.

In single crystals and surface grains of polycrystals, a PSB ends on the specimen surface in intrusions and extrusions (see Figure 1). This is due to close-enough positive and negative dislocations annihilating via cross-slip (for the screw components) or climb (for the edge components), which produces vacancies [24]. PSBs are composed of multiple parallel layers which are induced by inter-dislocation attractive and repulsive forces.

In polycrystalline materials, dislocation arrangements are similar to those in single crystals, except that the dislocations are impeded by the Grain Boundaries (GBs) resulting in pile-up [24].

Crack initiation can also occur within a grain (not at the GB), although this is generally the case for materials with defects, inhomogeneities or large grain size. In superalloys, improvements in processing have led to a significant reduction in material defects and therefore reduced intra-granular initiation [31]. It has been experimentally shown that during initiation, micro-cracks can develop along the GB, along the PSB or along both depending on the angles formed by the directions of the GB, of the PSB and the loading direction [32].

Tanaka and Mura developed a micromechanical model for fatigue crack initiation [8]. Their theory is based on dislocation pile-up at the PSB-GB interface. Forward and reverse plastic flow is modeled by dislocations with different signs moving on two closely located layers, and it is assumed that their movement is irreversible.

Each cycle induces an increase of the plastic strain energy per unit width in each layer of the PSB:

$$\Delta U = \frac{\pi(1-\nu)}{8G}(\Delta\tau - 2k)^2 d^2 \tag{1}$$

Where $\Delta\tau$ is the shear stress range, k is the frictional stress, d is the PSB length, ν is the Poisson's ratio and G is the shear modulus. Frictional stress is the critical stress that needs to be overcame in order to let the dislocations slip.

The definition of crack initiation depends on the length scale being considered [33]. From a microscopic point of view, a crack corresponds to the local overcoming of interatomic cohesive forces and thus, the creation of new surfaces. From a mesoscopic scale, an initiation can be considered when a crack reaches a significant size compared to the grain size order. At this length scale, crack propagation depends on microstructural features such as grain orientations and grain boundaries [33]. This is no longer the case at a macroscopic length scale where the material can be considered as homogeneous and thus crack propagation rate can be modeled by Linear Elastic Fracture Mechanics (LEFM) for example.

Tanaka and Mura originally considered that a crack initiation occurs when the accumulated energy at layer I and layer II reaches specific fracture energy of a crack of the same length as the PSB. This leads to:

$$U_I + U_{II} = 2N_i\Delta U = 2dW_s \tag{2}$$

With N_i the fatigue crack threshold (number of cycles) and W_s the specific fracture energy for a unit area.

Substituting Equation 1 into Equation 2 and rearranging gives:

$$N_i = \frac{8GW_s}{\pi(1-\nu)d(\Delta\tau - 2k)^2} \tag{3}$$

Improvements of the model have been proposed by Mura and Nakasone [34, 35] who used Gibb's free energy. Other authors proposed variants of this model with the use of additional parameters such as Burgers vector [36] or the PSB width [37]. The original model has nevertheless received great popularity within the scientific community because it captures the essence of crack initiation via slip and accumulation of dislocations. Several studies have been able to correlate the Tanaka-Mura fatigue crack initiation model with

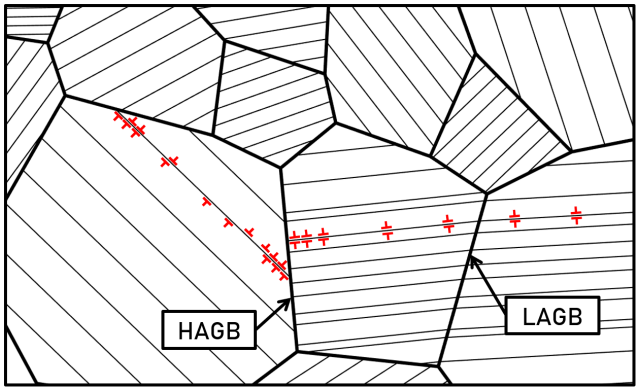

Figure 2: Dislocations moving along Persistent Slip Bands, piling-up at High-Angle Grain Boundaries (HAGBs) and passing trough Low-Angle Grain Boundaries (LAGBs).

experimental results [17, 38, 39, 40, 41]. Cheng and Cheng compared the same type of model with experimental results in RCF conditions [42, 43].

At first, GBs were considered as impenetrable [10] but later, Blochwitz et al. showed that misorientation of adjacent grains have an influence on PSB-GB interaction [11]. Zhang and Wang [13, 14, 15] showed that PSBs can pass through Low Angle Grain Boundaries (LAGBs). Therefore, cracking does not occur at these GBs. LAGBs are defined as a misorientation between adjacent grains of less than $\theta_c = 15°$ [24]. Concerning High Angle Grain Boundaries (HAGBs), dislocations pile-up at the PSB-GB interface, building up stress concentration over the repeated loading cycles, eventually leading to crack initiation (see Figure 2).

As discussed, fatigue crack initiation results from the accumulation of plastic strain due to dislocation slip along PSBs and interacting with the microstructure. In the next section a numerical model for crack initiation in RCF is presented.

3. Model

Two variables need to be calculated in order to use Tanaka-Mura's law for crack initiation. The first one is shear stress range $\Delta\tau$ which has been previously calculated according to different methods in an isotropic model [23]. In this present paper, the use of cubic elasticity in a 2D polycrystalline model opens new perspectives. Secondly, PSB length d which has been previously approximated by the grain size can now be calculated in the relevant directions and eventually allowing PSBs to pass through LAGBs.

The numerical model used in this study is similar to the previous one [23] on multiple aspects. It uses a moving contact pressure to simulate the rolling contact onto the surface of the material. A loading cycle is represented by the displacement of the contact pressure from $x = -4a$ to $x = 4a$, with contact half-width a (see Figure 3). The simulation is performed for dry contact, in order to analyze the most severe case of damage [44]. In order to initiate surface and sub-surface cracks, two surface conditions are simulated:

- Smooth contact surface ($p = p_{hertz}$)
- Dented contact surface ($p = p_{hertz} + \Delta p_{dent}$)

p_{hertz} is calculated using Hertz contact theory [45] and Δp_{dent} is calculated using Coulon et al. [44, 46]. The contact characteristics are given Table 1.

Table 1
Contact and dent characteristics.

Characteristic	Notation	Unit	Value
Half-width	a	$[\mu m]$	615
Max contact pressure	p_0	$[MPa]$	2100
Dent diameter	ϕ	$[\mu m]$	250
Dent depth	d_{th}	$[\mu m]$	37

Stresses are calculated by FEM computation with quasi-static conditions for each incremental position of the contact pressure (274 increments). Stress components σ_x, σ_y, σ_z and τ_{xy} are obtained with plane strain assumptions. An area of analysis with a width of $2.5a$ is embedded into a wider body, large enough to behave as a semi-infinite body (see Figure 3). The polycrystalline geometry of the area of analysis has been generated using the open access software package `Neper` [47, 48, 49] which uses Voronoi tessellation algorithms. The mean grain size is equal to $25\mu m$ and the size distribution follow a log-normal law with a standard deviation of $11\mu m$. Each grain is meshed into quadratic quadrangles.

In this study, the anisotropic character of each crystal of the model is based on Noyel [50]. Applying crystal elasticity to each grain with random crystal orientations allows to preserve the material macroscopic isotropic behavior. With a large enough number of randomly oriented grains, the macroscopic behavior of the locally-anisotropic mesoscopic model converges to the behavior of an isotropic material. It has been previously verified that the values used in this paper are relevant for both local and global considerations [51]. Even though RCF models could be applied to rolling element bearings, gears or railway tracks that can be composed of several material constituents, Noyel considered the main material constituent: α-iron. The crystal coordinate system (x_g, y_g) is aligned with the atoms of the crystal lattice of the grain (see Figure 4).

Cubic elasticity stiffness matrix $[C]$ (Equation 4) is described by three independent constants C_{11}, C_{12}, and C_{44}. The values defined by Courtney [52] are used in this study (see Table 2).

$$\begin{Bmatrix} \sigma_x \\ \sigma_y \\ \sigma_z \\ \tau_{yz} \\ \tau_{xz} \\ \tau_{xy} \end{Bmatrix} = \begin{bmatrix} C_{11} & C_{12} & C_{12} & 0 & 0 & 0 \\ C_{12} & C_{11} & C_{12} & 0 & 0 & 0 \\ C_{12} & C_{12} & C_{11} & 0 & 0 & 0 \\ 0 & 0 & 0 & C_{44} & 0 & 0 \\ 0 & 0 & 0 & 0 & C_{44} & 0 \\ 0 & 0 & 0 & 0 & 0 & C_{44} \end{bmatrix} \times \begin{Bmatrix} \varepsilon_x \\ \varepsilon_y \\ \varepsilon_z \\ 2\varepsilon_{yz} \\ 2\varepsilon_{xz} \\ 2\varepsilon_{xy} \end{Bmatrix} \quad (4)$$

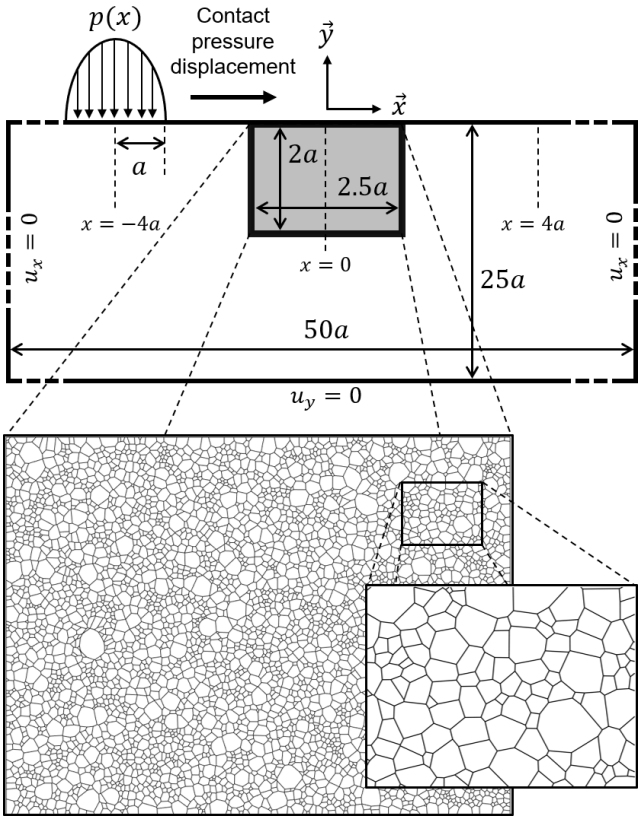

Figure 3: Model dimensions and polycrystalline geometry.

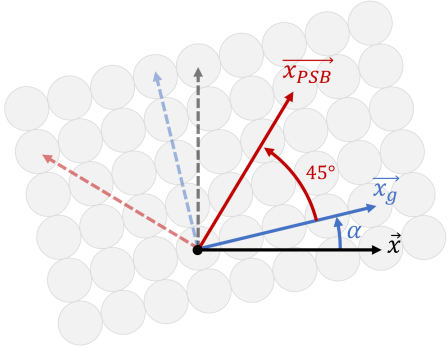

Figure 4: Global coordinate system (x, y), grain local coordinate system (x_g, y_g), slip local coordinate system (x_{PSB}, y_{PSB}).

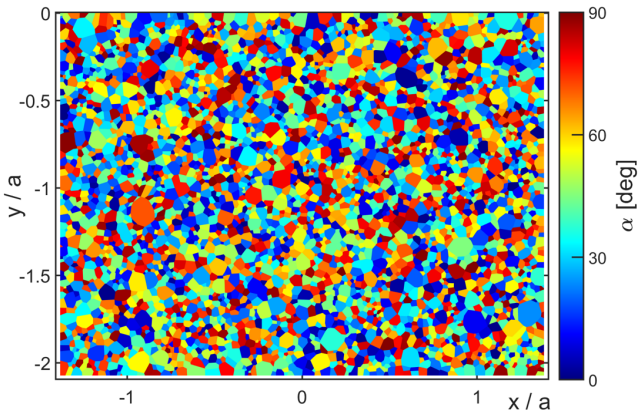

Figure 5: Distribution of grains orientations α.

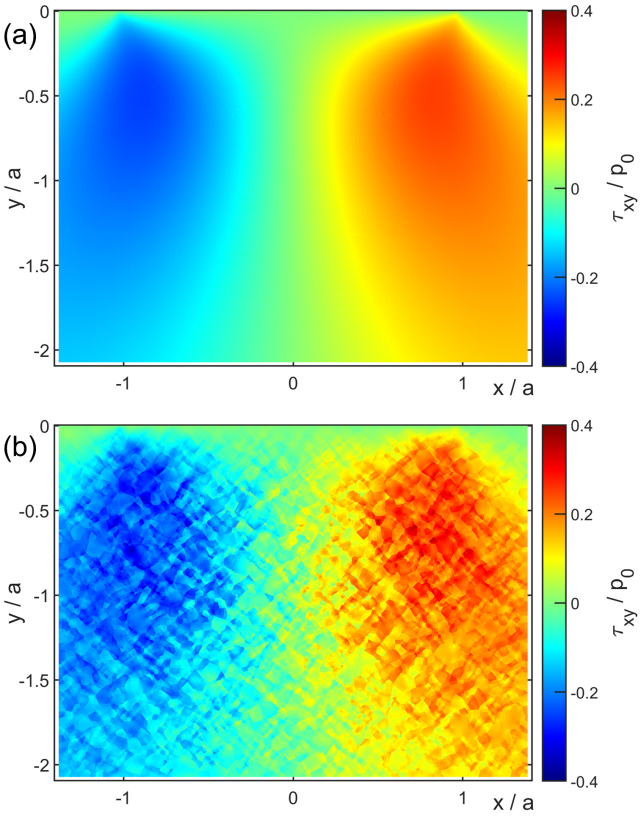

Figure 6: Orthogonal shear stress τ_{xy} for a centered contact pressure in smooth surface condition for (a) isotropic properties, (b) cubic elasticity properties.

Table 2
Stiffness matrix components of α-iron [50].

C_{11}	C_{12}	C_{44}
237 GPa	141 GPa	116 GPa

The same type of crystal cubic elasticity has been used in RCF mesoscopic models in previous works [53, 54, 55, 56].

An in-plane orientation is assigned to each grain. These orientations are defined by random angles α varying between 0° and 90° which represents the rotation angle around z axis between the global coordinate system (x, y) and the grain local coordinate system (x_g, y_g) (see Figure 5).

FEM computation provides stress distribution at each point of the meshed geometry and for each position of the moving contact pressure. In order to illustrate the effect of cubic elasticity on the stress field, Figure 6 shows the orthogonal shear stress τ_{xy} for a centered contact pressure under smooth surface condition for (a) isotropic properties and (b) cubic elasticity properties.

Next section develops fatigue crack initiation simulation

in RCF using the previously addressed model and single-grain PSBs.

4. Crack Initiation with Single-Grain PSBs

The Tanaka-Mura micromechanical model considers shear stress range $\Delta\tau$ as a variable influencing crack initiation. As discussed in section 2, shear stress produces dislocations, induces slip and is therefore the cause of strain energy accumulation. Multiple options exist concerning the calculation of the shear stress: maximum shear stress, orthogonal shear stress, octahedral shear stress, etc. These different possibilities are compared and discussed in a previous study [23]. Since grain orientations are considered in this paper, a more physical approach is possible: calculate shear stress range directly in the slip directions. This is called resolved shear stress.

In this study, only in-plane slip systems are considered. Since stress components are calculated for a bcc material, the possible slip systems are positioned at $+45°$ and $-45°$ from the grain local coordinate system (see Figure 4).

After changing coordinate system, it can be shown that resolved shear stress along x_{PSB} is given by:

$$\tau_{x_{PSB}} = \tau_{xy} \sin 2\alpha + \frac{1}{2}(\sigma_x - \sigma_y) \cos 2\alpha \tag{5}$$

$\tau_{x_{PSB}}$ is the opposite of $\tau_{y_{PSB}}$ for each contact pressure incremental position. Therefore, resolved shear stress range $\Delta\tau$ is identical for every PSBs inside a grain whether the PSB is oriented according to x_{PSB} or y_{PSB}.

$\Delta\tau$ is calculated using the maximum and minimum of τ_{PSB} during the displacement of the moving contact pressure:

$$\Delta\tau = max(\tau_{PSB}) - min(\tau_{PSB}) \tag{6}$$

σ_x, σ_y, and τ_{xy} correspond to averaged values of each element of a grain and α is the grain orientation angle which has already been used is the FEM anisotropic computation.

Figure 7 shows the resolved shear stress range $\Delta\tau$ for the smooth contact and the dented contact.

Material parameters can take different values depending on bearing steel grades. Material property values that are used in the present study [23] are in Table 3. The value of W_s was determined by Tryon et al. [38] and the value of k can be found in Kamimura et al.'s review [57].

Table 3
Tanaka-Mura model parameters for bearing steel.

Parameter	Notation	Unit	Value
Shear modulus	G	$[GPa]$	80
Poisson's ratio	ν	$[-]$	0.3
Fracture energy [38]	W_s	$[kJ/m^2]$	440
Frictional stress [57]	k	$[MPa]$	390

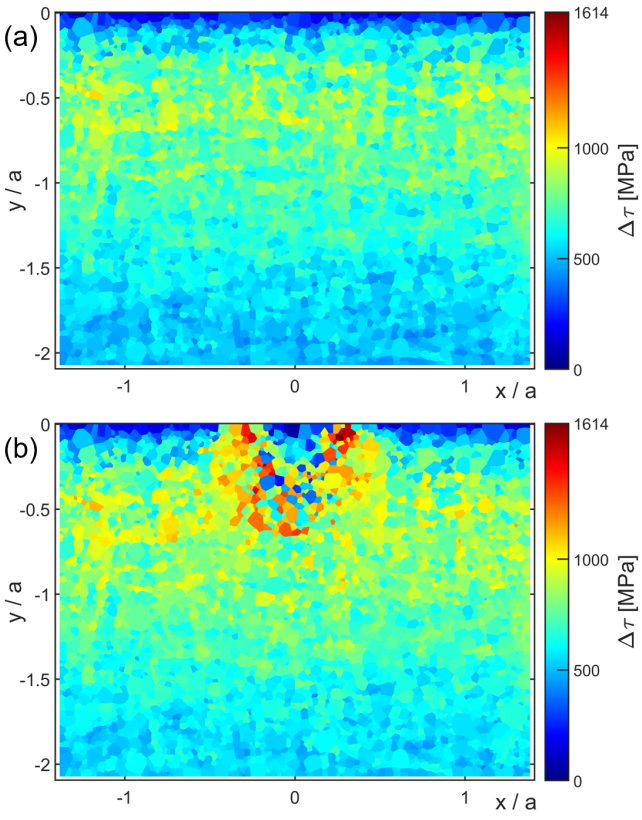

Figure 7: Resolved shear stress range for (a) smooth surface, (b) dented surface.

Several crack initiation criteria can be considered depending on the length scale and the physics considered in a model. Tanaka and Mura choose to consider a grain-scale (i.e. mesoscopic) criterion for crack initiation. This results in initiation of cracks of the same length as the PSBs that contributed to strain energy accumulation. In other words, they predicted that a PSB converts into a crack when sufficient energy is piled-up. Other models could arguably consider other hypotheses concerning the length scale of the initiated cracks, however, this study proceeds with the initial mesoscopic hypothesis.

The model which is developed in this paper is varied into three different combinations of hypotheses. These model variants are defined in Table 4. Model A is obtained with the simplest hypotheses, grain properties are isotropic, $\Delta\tau$ is calculated in the direction that maximizes it and PSB length is approximated by grain size. This first model has already been used in the previous study [23]. Model B differs from previous one because grains are considered as anisotropic and crystal orientations are randomly distributed. This allows computation of $\Delta\tau$ in the slip directions as described in section 3. At this point, there is no multi-grain PSB. PSB lengths are approximated by grain size by finding the longest segment in the direction of $\Delta\tau$ of each grain. Model C, which considered more advanced hypotheses, is discussed in the next section.

Figure 8 shows a comparison between models A and B

Table 4
Hypotheses of the different models.

Model	A	B	C
Grain properties	Isotropy	Cubic elasticity	Cubic elasticity
$\Delta\tau$ direction	Maximizes ($\Delta\tau_{meso}$)	Slip direction ($\Delta\tau_{PSB}$)	Slip direction ($\Delta\tau_{PSB}$)
PSB length	Grain size	Grain size	Multi-grain PSB

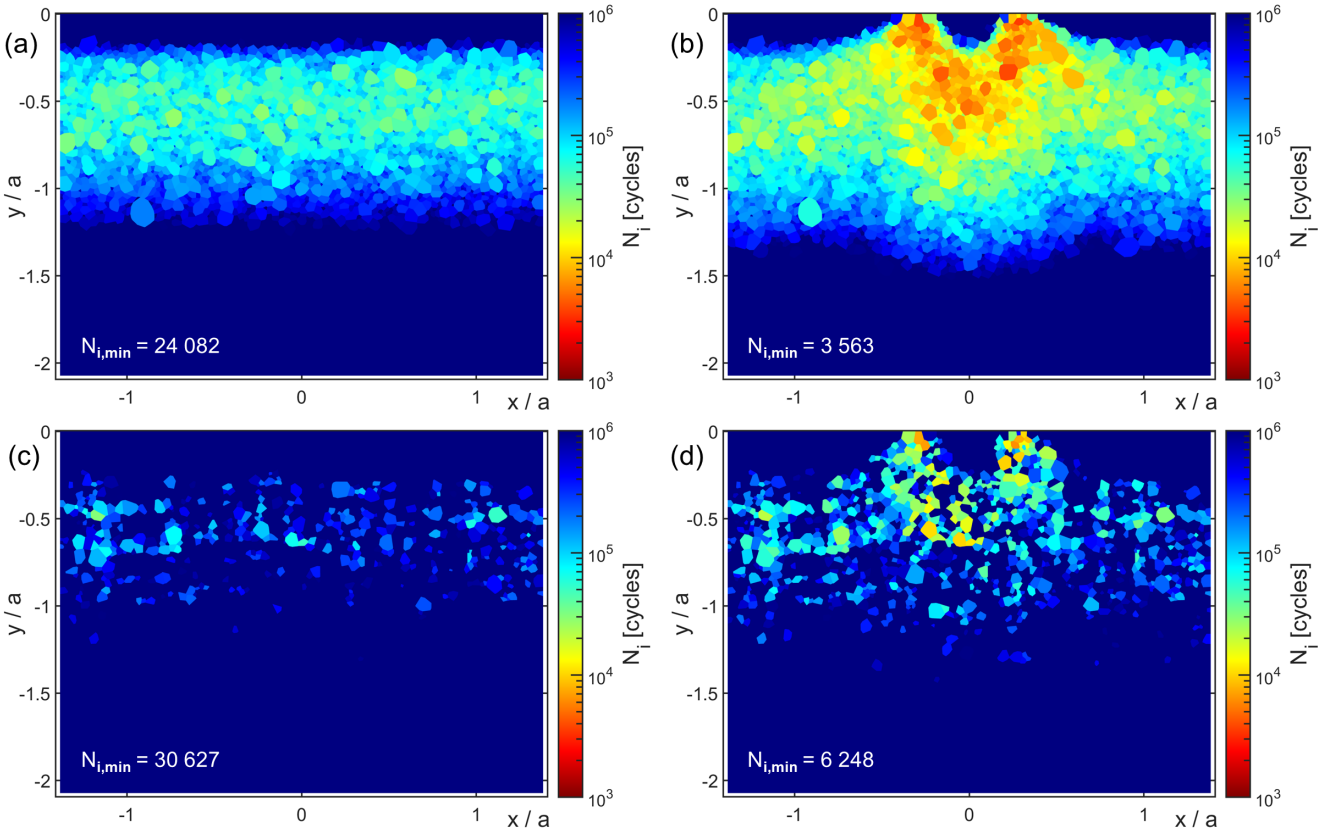

Figure 8: Fatigue crack threshold for (a,b) model A, (c,d) model B, in the case of (a,c) smooth surface, (b,d) dented surface.

on the number of cycles required for crack initiation. Model A is more critical than model B. This is consistent since in model A, shear stress range $\Delta\tau$ is calculated in the direction that maximizes it [23]. In model A, N_i distribution basically depends on the grain position. For instance, in the case of the smooth surface, the value of N_i is highly influenced by the depth of the grain. Grain size differentiates adjacent grains that are at the same depth. N_i distribution has more of a random aspect in model B since crack initiation depends not only on grain size, but also on grain orientation which can be very favorable or very unfavorable towards crack initiation. This leads to a more scattered distribution both in the case of the smooth surface and in the case of the dented surface.

Thus far, PSB length d was approximated by grain size. In the next section, it is proposed to model multi-grain PSBs in order to get a more physically based approach.

5. Crack Initiation with Multi-Grain PSBs

It is possible to estimate the length of real PSBs by taking into account the misorientations between grains. As Tanaka-Mura's equation implies (see Equation 3), PSB length as an influence on fatigue crack initiation. Longest PSBs are more critical for material due to the larger amount of accumulated dislocations. This statement is consistent with the Hall-Petch relationship. As previously described in section 2, if the misorientation angle of two adjacent grains is small enough, dislocations can cross the GB which is therefore called a LAGB (see Figure 2). This phenomenon leads to the formation of multi-grain PSBs. In this section, an algorithm to model multi-grain PSBs in polycrystals is proposed.

A grid is generated inside each grain, following the two possible slip directions x_{PSB} and y_{PSB} of the slip local coordinate system (see Figure 4). In the algorithm, the number of PSBs per grain and per direction can be control by parameter n_{PSB}. When a line of the grid crosses a GB, the intersection

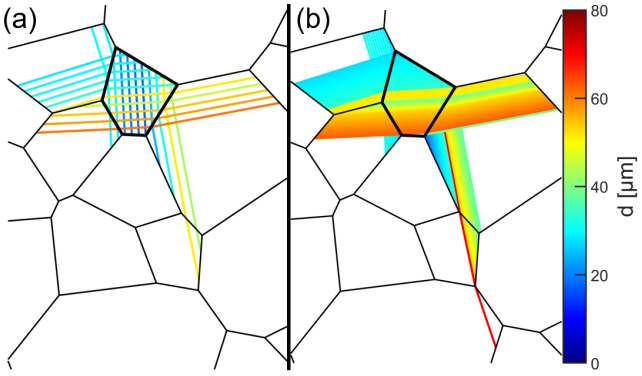

Figure 9: PSB passing though GBs for (a) $n_{PSB} = 10$, (b) $n_{PSB} = 100$.

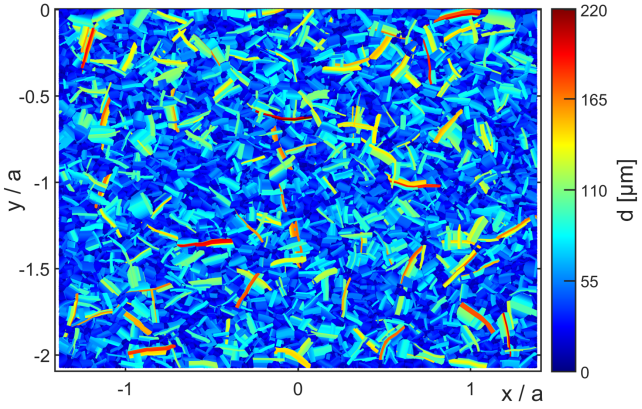

Figure 10: PSB field in the polycristalline geometry of the area of analysis using $n_{PSB} = 100$.

point is found, both adjacent grains are identified and if their misorientation is lower than the critical misorientation angle $\theta_c = 15°$ [24], the line passes through the GB following the new slip direction. A PSB which has been generated following the direction x_{PSB} of the first grain can be extended following either x_{PSB} or y_{PSB} of a second grain as long as the angular difference between the first and the second direction is lower than θ_c. Figure 9 shows the algorithm applied to one grain only: in case that $n_{PSB} = 10$ (a), in case that $n_{PSB} = 100$ (b). In the second case, more PSB paths are considered as an additional grain can be reached, leading to longer PSBs.

When the algorithm is applied to each grain of the analysis area, a PSB field is generated (see Figure 10). Each PSB is colored according to its length. In the present case, the longest PSB equals $220\mu m$ which corresponds to around 9 grains.

The number of cycles required for crack initiation can be calculated from the Tanaka-Mura model (Equation 3) using resolved shear stress range $\Delta\tau$, PSB length d and the material properties. The multiple segments of the PSBs are used in this calculation. Each segment contributes to the energy that is accumulated in a PSB. Building from Tanaka-Mura's principle, the total accumulated energy per cycle in a PSB

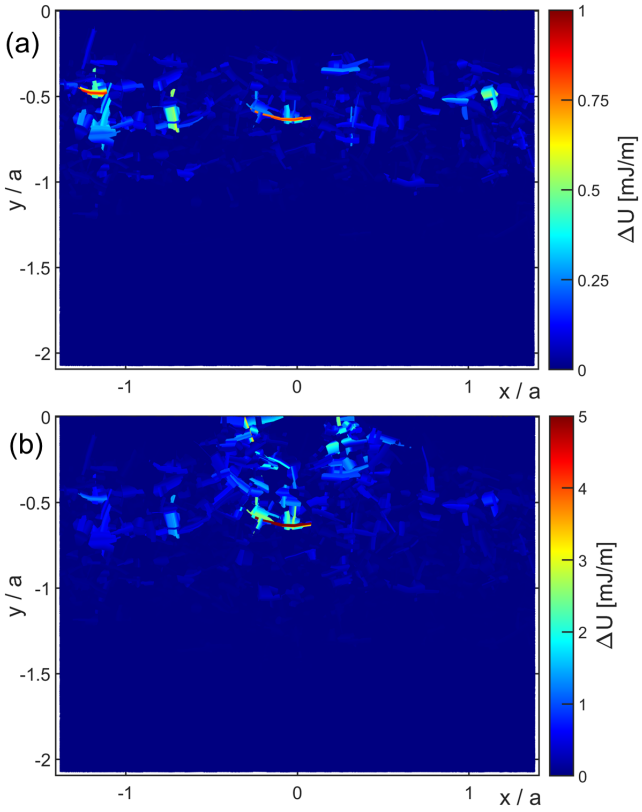

Figure 11: Accumulated strain energy per unit width per cycle for (a) smooth surface, (b) dented surface.

crossing n grains is:

$$\Delta U_{PSB} = \frac{\pi(1-\nu)}{8G} \sum_{g=1}^{n} (\Delta\tau_g - 2k)^2 d_g^2 \tag{7}$$

With $\Delta\tau_g$ the mean resolved shear stress range in the grain of the PSB segment g, and the length of the PSB segment d_g. Accumulated energy per cycle ΔU is shown Figure 11 for (a) smooth surface conditions and (b) dented surface conditions.

Considering the initiation of a crack of the same length as the PSB, the energy criterion is:

$$2N_{i,PSB}\Delta U_{PSB} = 2dW_s \tag{8}$$

With $N_{i,PSB}$ the number of cycles required to initiate a crack along the PSB, d the multi-grain PSB length and W_s the specific fracture energy for a unit area. This leads to:

$$N_{i,PSB} = \frac{8GW_s}{\pi(1-\nu)} \frac{\sum_{g=1}^{n} d_g}{\sum_{g=1}^{n} d_g^2(\Delta\tau_g - 2k)^2} \tag{9}$$

The assumption that a crack is initiated when the energy level reaches the requirement for cracking the entire PSB is still considered here. Even though an initiated crack is generally smaller than a PSB and then grows into a full PSB length [33], it is more convenient to start with Tanaka-Mura's original hypothesis as this model operates at a mesoscopic length scale.

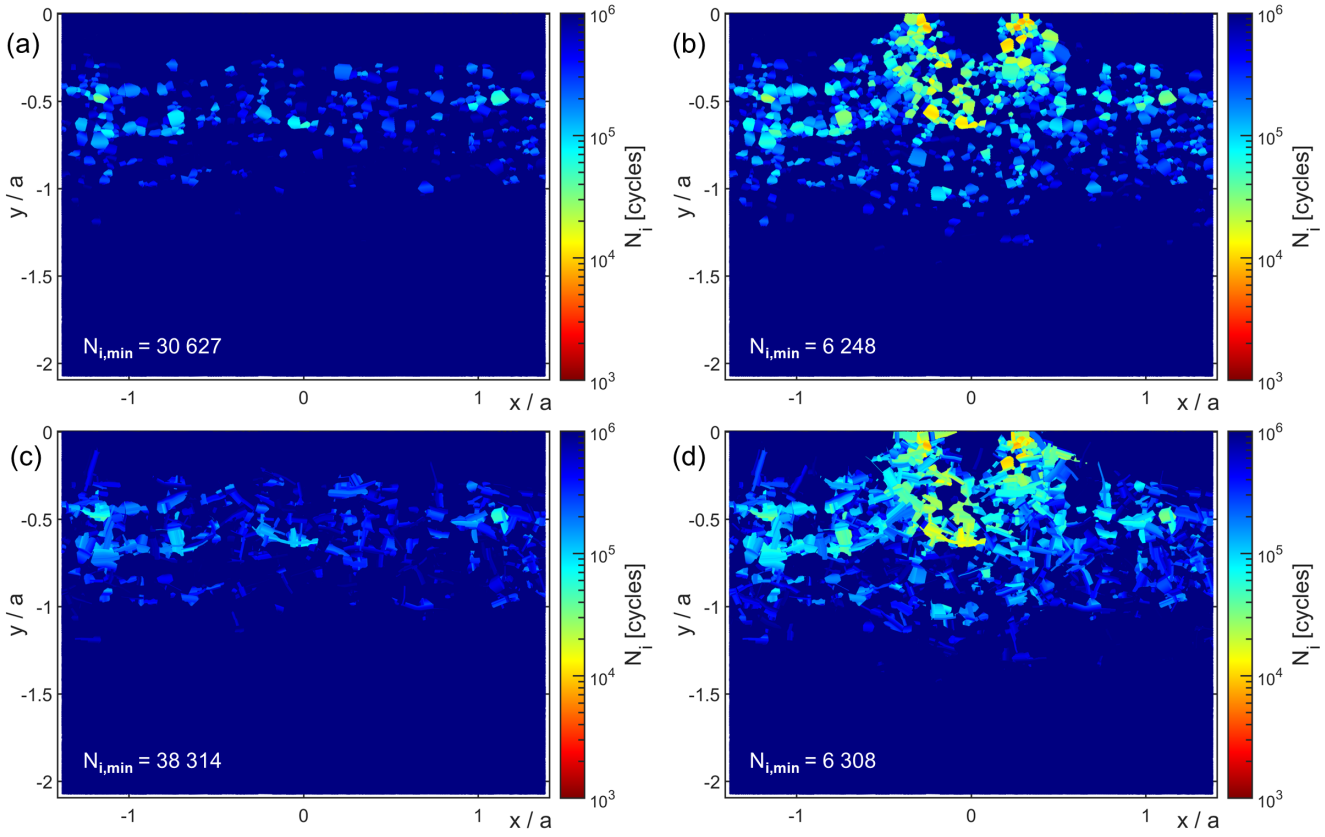

Figure 12: Fatigue crack threshold for (a,b) model B', (c,d) model C in the case of (a,c) smooth surface, (b,d) dented surface.

Figure 12 compares two models: models B' and C. Model B' is equivalent to model B but the representations are different. Contrary to model B in Figure 8 where only the value of the longest PSB is displayed, in model B' each PSB is displayed in order to compare it to model C. Hence model B' simulates the presence of PSBs without allowing for passing through GBs. In model C, passing through LAGBs is allowed, so that multi-grain PSBs are simulated. $n_{PSB} = 100$ has been found to be the convergence criterion to not have results depending on the number of PSBs per grain and per direction.

As expected, contact surface conditions have a predominant influence on fatigue crack threshold with either single-grain PSBs or multi-grain PSBs. A damaged surface highly decreases $N_{i,min}$.

There is a slight difference between the predictions of model B' (single-grain PSBs) and model C (multi-grain PSBs). Model B' is more critical (lower $N_{i,min}$) than model C. This can be explained by the fact that energy accumulation needs to reach a level which is proportional to the PSB length in order to initiate a crack. Even though longer PSBs accumulate more energy than smaller PSBs (at the same stress level), they also need more energy to be entirely cracked.

Average depth of early crack initiation ($N_i < 10 \times N_{i,min}$) in the case of a smooth surface (Hertzian contact pressure) is equal to:

- $y_m = -0.62a$ for model A
- $y_m = -0.56a$ for model B
- $y_m = -0.57a$ for model C

Chen et al. found experimentally an average value of $y_m = -0.522a$ [58, 59]. This experimental value was obtained with only 13 measurements of crack depth but averages are still similar. This agreement between experimental and numerical results for Hertzian type contacts allows a reasonable confidence in the method developed in the present study and in its application to other surface conditions.

6. Conclusions

In this study, a 2D polycrystalline model has been developed using crystal anisotropy in order to compute realistic stress distribution in the surface of a material exposed to rolling contact pressure. Two independent cases have been considered: smooth and dented surface conditions. These cases could be combined by summing the different accumulated energies. Benefits of these assumptions over a previous isotropic model on crack initiation are shown using Tanaka-Mura's approach in order to account for the fundamental mechanics of fatigue, i.e. strain energy accumulation through dislocation formation and slip.

The main interest of this paper lies in the modeling of multi-grain PSBs, allowing a more realistic simulation in agreement with experimental observations showing PSBs passing through low angle grain boundaries.

As material parameters are still an important source of uncertainty, validation of the model could be made by comparing the results with experiments. These correlations would provide more confidence, in particular concerning fracture energy W_s and frictional stress k. Further improvements could be made concerning the material behavior by modeling crystal plasticity or material heterogeneities. Grain size variation depending on depth could be considered as well as macroscopic anisotropy induced by crystal orientation texture. Concerning the surface, friction and roughness could be modeled. In-plane grain orientations are also a questionable assumption. A 3D model would help to solve this issue along with modeling the PSBs in a 3D space.

References

[1] A. Wöhler, *Über die festigkeitsversuche mit eisen und stahl*. Ernst & Korn, 1870.

[2] S. S. Manson, *Behavior of materials under conditions of thermal stress*, vol. 2933. National Advisory Committee for Aeronautics, 1953.

[3] L. F. Coffin, "A study of the effects of cyclic thermal stresses on a ductile metal," *Transactions of the American Society of Mechanical Engineers, New York*, vol. 76, pp. 931–950, 1954.

[4] G. Lundberg, "Dynamic capacity of rolling bearings," *IVA Handlingar*, vol. 196, p. 12, 1947.

[5] A. G. Pålmgren, "Die lebensdauer von kugellagern," *Zeitschrift des Vereinesdeutscher Ingenierure*, vol. 68, no. 14, pp. 339–341, 1924.

[6] F. Sadeghi, B. Jalalahmadi, T. S. Slack, N. Raje, and N. K. Arakere, "A Review of Rolling Contact Fatigue," *Journal of Tribology*, vol. 131, 09 2009. 041403.

[7] R. S. Zhou, H. S. Cheng, and T. Mura, "Micropitting in Rolling and Sliding Contact Under Mixed Lubrication," *Journal of Tribology*, vol. 111, pp. 605–613, 10 1989.

[8] K. Tanaka and T. Mura, "A Dislocation Model for Fatigue Crack Initiation," *Journal of Applied Mechanics*, vol. 48, pp. 97–103, 03 1981.

[9] J. A. Ewing and J. C. W. Humfrey, "The fracture of metals under repeated alternations of stress," *Proceedings of the Royal Society of London*, vol. 71, p. 79, 1902.

[10] G. Dörr and C. Blochwitz, "Microcracks in fatigued fcc polycrystals by interaction between persistent slip bands and grain boundaries," *Crystal Research and Technology*, vol. 22, no. 1, pp. 113–121, 1987.

[11] C. Blochwitz, J. Brechbühl, and W. Tirschler, "Misorientation measurements near grain boundary cracks after fatigue tests," *Strength of materials*, vol. 27, no. 1-2, pp. 3–13, 1995.

[12] C. Blochwitz, J. Brechbühl, and W. Tirschler, "Analysis of activated slip systems in fatigue nickel polycrystals using the ebsd-technique in the scanning electron microscope," *Materials Science and Engineering: A*, vol. 210, no. 1, pp. 42 – 47, 1996.

[13] Z. Zhang and Z. Wang, "Comparison of fatigue cracking possibility along large- and low-angle grain boundaries," *Materials Science and Engineering: A*, vol. 284, no. 1, pp. 285 – 291, 2000.

[14] Z. Zhang and Z. Wang, "Relationship between the fatigue cracking probability and the grain-boundary category," *Philosophical Magazine Letters*, vol. 80, no. 7, pp. 483–488, 2000.

[15] Z. Zhang and Z. Wang, "Dependence of intergranular fatigue cracking on the interactions of persistent slip bands with grain boundaries," *Acta Materialia*, vol. 51, no. 2, pp. 347 – 364, 2003.

[16] A. Brückner-Foit and X. Huang, "Numerical simulation of microcrack initiation of martensitic steel under fatigue loading," *International Journal of Fatigue*, vol. 28, no. 9, pp. 963 – 971, 2006. Fatigue lifetime prediction of metals based on microstructural behaviour.

[17] A. Bruckner-Foit and X. Huang, "On the determination of material parameters in crack initiation laws," *Fatigue & Fracture of Engineering Materials & Structures*, vol. 31, no. 11, pp. 980–988, 2008.

[18] S. Toyoda, H. Kimura, Y. Kawabata, S. Hashimoto, N. Yoshihara, and J. Sakai, "Numerical simulation of fatigue crack initiation in thin-walled high strength steel as modeled by voronoi-polygons," *ISIJ international*, vol. 50, no. 11, pp. 1695–1701, 2010.

[19] P.-M. Hilgendorff, A. Grigorescu, M. Zimmermann, C.-P. Fritzen, and H.-J. Christ, "Simulation of irreversible damage accumulation in the very high cycle fatigue (vhcf) regime using the boundary element method," *Materials Science and Engineering: A*, vol. 575, pp. 169 – 176, 2013.

[20] F. Briffod, T. Shiraiwa, and M. Enoki, "Microstructure modeling and crystal plasticity simulations for the evaluation of fatigue crack initiation in α-iron specimen including an elliptic defect," *Materials Science and Engineering: A*, vol. 695, pp. 165 – 177, 2017.

[21] A. V. Olver, "The mechanism of rolling contact fatigue: An update," *Proceedings of the Institution of Mechanical Engineers, Part J: Journal of Engineering Tribology*, vol. 219, no. 5, pp. 313–330, 2005.

[22] N. Raje, T. Slack, and F. Sadeghi, "A discrete damage mechanics model for high cycle fatigue in polycrystalline materials subject to rolling contact," *International Journal of Fatigue*, vol. 31, no. 2, pp. 346 – 360, 2009.

[23] L. Fourel, E. Bossy, J.-P. Noyel, X. Kleber, and F. Ville, "Towards a grain-scale modeling of crack initiation in rolling contact fatigue - part 1: Shear stress considerations," *Submitted*, 2021.

[24] M. D. Sangid, "The physics of fatigue crack initiation," *International Journal of Fatigue*, vol. 57, pp. 58 – 72, 2013. Fatigue and Microstructure: A special issue on recent advances.

[25] Z. Basinski and S. Basinski, "Fundamental aspects of low amplitude cyclic deformation in face-centred cubic crystals," *Progress in Materials Science*, vol. 36, pp. 89 – 148, 1992.

[26] J. C. Grosskreutz, "The mechanisms of metal fatigue (i)," *physica status solidi (b)*, vol. 47, no. 1, pp. 11–31, 1971.

[27] P. Lukáš and L. Kunz, "Role of persistent slip bands in fatigue," *Philosophical Magazine*, vol. 84, no. 3-5, pp. 317–330, 2004.

[28] F. Boehme, K. Hidaka, and J. Weertman, "Psb observation in copper fatigued at one half the melting temperature," *Scripta Metallurgica et Materialia*, vol. 24, no. 12, pp. 2341 – 2346, 1990.

[29] N. H. Forster, L. Rosado, W. P. Ogden, and H. K. Trivedi, "Rolling contact fatigue life and spall propagation characteristics of aisi m50, m50 nil, and aisi 52100, part iii: Metallurgical examination," *Tribology Transactions*, vol. 53, no. 1, pp. 52–59, 2009.

[30] S. Medina, A. Olver, and B. Shollock, "Development of rolling contact damage in two bronze alloys," in *Transient Processes in Tribology* (G. Dalmaz, A. Lubrecht, D. Dowson, and M. Priest, eds.), vol. 43 of *Tribology Series*, pp. 619 – 627, Elsevier, 2003.

[31] M. D. Sangid, H. J. Maier, and H. Sehitoglu, "The role of grain boundaries on fatigue crack initiation – an energy approach," *International Journal of Plasticity*, vol. 27, no. 5, pp. 801 – 821, 2011.

[32] Y. Li, *Amorçage de fissures en fatigue dans un acier 304L: influence de la microstructure et d'un chargement d'amplitude variable*. PhD thesis, Ecole Centrale Paris, 2 2012.

[33] U. Krupp, *Fatigue crack propagation in metals and alloys: microstructural aspects and modelling concepts*. John Wiley & Sons, 2007.

[34] T. Mura and Y. Nakasone, "A theory of fatigue crack initiation in solids," *Journal of Applied Mechanics*, vol. 57, pp. 1–6, 1990.

[35] T. Mura, "A theory of fatigue crack initiation," *Materials Science and Engineering: A*, vol. 176, no. 1, pp. 61 – 70, 1994.

[36] X. Wu, "A fatigue crack nucleation model for anisotropic materials," *Fatigue & Fracture of Engineering Materials & Structures*, vol. 42, no. 1, pp. 387–393, 2019.

[37] K. S. Chan, "A microstructure-based fatigue-crack-initiation model," *Metallurgical and Materials Transactions A*, vol. 34, no. 1, pp. 43–58, 2003.

[38] R. Tryon and T. Cruse, "A reliability-based model to predict scatter in fatigue crack nucleation life," *Fatigue & Fracture of Engineering Materials & Structures*, vol. 21, no. 3, pp. 257–267, 1998.

[39] N. Jezernik, J. Kramberger, T. Lassen, and S. Glodez, "Numerical modelling of fatigue crack initiation and growth of martensitic steels," *Fatigue & Fracture of Engineering Materials & Structures*, vol. 33,

no. 11, pp. 714–723, 2010.

[40] J. Kramberger, N. Jezernik, P. Göncz, and S. Glodež, "Extension of the tanaka–mura model for fatigue crack initiation in thermally cut martensitic steels," *Engineering Fracture Mechanics*, vol. 77, no. 11, pp. 2040 – 2050, 2010. International Conference on Crack Paths 2009.

[41] T. Hoshide and K. Kusuura, "Life prediction by simulation of crack growth in notched components with different microstructures and under multiaxial fatigue," *Fatigue & Fracture of Engineering Materials & Structures*, vol. 21, no. 2, pp. 201–213, 1998.

[42] W. Cheng, H. S. Cheng, T. Mura, and L. M. Keer, "Micromechanics Modeling of Crack Initiation Under Contact Fatigue," *Journal of Tribology*, vol. 116, pp. 2–8, 01 1994.

[43] W. Cheng and H. S. Cheng, "Semi-Analytical Modeling of Crack Initiation Dominant Contact Fatigue Life for Roller Bearings," *Journal of Tribology*, vol. 119, pp. 233–240, 04 1997.

[44] S. Coulon, F. Ville, and A. A. Lubrecht, "Effect of a dent on the pressure distribution in dry point contacts," *Journal of Tribology*, vol. 124, pp. 220–223, 03 2001.

[45] K. Johnson, "Contact mechanics and the wear of metals," *Wear*, vol. 190, no. 2, pp. 162 – 170, 1995.

[46] S. Coulon, F. Ville, and A. Lubrecht, "An abacus for predicting the rolling contact fatigue life reduction due to debris dents," in *Boundary and Mixed Lubrication* (D. Dowson, M. Priest, G. Dalmaz, and A. Lubrecht, eds.), vol. 40 of *Tribology Series*, pp. 283 – 293, Elsevier, 2002.

[47] R. Quey, P. Dawson, and F. Barbe, "Large-scale 3d random polycrystals for the finite element method: Generation, meshing and remeshing," *Computer Methods in Applied Mechanics and Engineering*, vol. 200, no. 17, pp. 1729 – 1745, 2011.

[48] R. Quey and L. Renversade, "Optimal polyhedral description of 3d polycrystals: Method and application to statistical and synchrotron x-ray diffraction data," *Computer Methods in Applied Mechanics and Engineering*, vol. 330, pp. 308 – 333, 2018.

[49] R. Quey, A. Villani, and C. Maurice, "Nearly uniform sampling of crystal orientations," *Journal of Applied Crystallography*, vol. 51, pp. 1162–1173, Aug 2018.

[50] J.-P. Noyel, F. Ville, P. Jacquet, A. Gravouil, and C. Changenet, "Development of a granular cohesive model for rolling contact fatigue analysis: Crystal anisotropy modeling," *Tribology Transactions*, vol. 59, no. 3, pp. 469–479, 2016.

[51] J.-P. Noyel, *Analyse de l'initiation de fissures en fatigue de contact : Approche mésoscopique*. Theses, INSA de Lyon, Dec. 2015.

[52] T. Courtney, *Mechanical Behavior of Materials: Second Edition*. Waveland Press, 2005.

[53] N. R. Paulson, J. A. Bomidi, F. Sadeghi, and R. D. Evans, "Effects of crystal elasticity on rolling contact fatigue," *International Journal of Fatigue*, vol. 61, pp. 67–75, 2014.

[54] A. Vijay and F. Sadeghi, "A continuum damage mechanics framework for modeling the effect of crystalline anisotropy on rolling contact fatigue," *Tribology International*, vol. 140, p. 105845, 2019.

[55] B. Zhang, A. F. Quiñonez, and C. H. Venner, "Effect of material anisotropy on rolling contact fatigue life under dry and lubricated point contact conditions: A numerical study," *Tribology International*, vol. 152, p. 106584, 2020.

[56] T. Beyer, T. Chaise, J. Leroux, F. Sadeghi, and D. Nelias, "A method to model crystalline anisotropy in contact using semi-analytical method," *Tribology International*, vol. 152, p. 106429, 2020.

[57] Y. Kamimura, K. Edagawa, and S. Takeuchi, "Experimental evaluation of the peierls stresses in a variety of crystals and their relation to the crystal structure," *Acta Materialia*, vol. 61, no. 1, pp. 294 – 309, 2013.

[58] L. Chen, Q. Chen, and E. S, "Study on initiation and propagation angles of subsurface cracks in gcr15 bearing steel under rolling contact," *Wear*, vol. 133, no. 2, pp. 205 – 218, 1989.

[59] Q. Chen, E. Shao, D. Zhao, J. Guo, and Z. Fan, "Measurement of the critical size of inclusions initiating contact fatigue cracks and its application in bearing steel," *Wear*, vol. 147, no. 2, pp. 285 – 294, 1991.